# Origin of magnetism in cobalt-doped indium tin oxide thin films

A. M. H. R. Hakimi,* F. Schoofs, R. Bali, N. A. Stelmashenko, and M. G. Blamire
*Department of Materials Science and Metallurgy, University of Cambridge, Pembroke Street, Cambridge CB3 9EU, United Kingdom*

S. Langridge
*Science and Technology Facilities Council, Rutherford Appleton Laboratory, Harwell Science and Innovation Campus, Didcot OX11 OQX, United Kingdom*

S. A. Cavill, G. van der Laan, and S. S. Dhesi
*Diamond Light Source, Harwell Science and Innovation Campus, Diamond House, Chilton, Didcot, Oxfordshire OX11 0DE, United Kingdom*

(Received 25 February 2010; revised manuscript received 13 August 2010; published 20 October 2010)

We report an x-ray absorption spectroscopy (XAS) and x-ray magnetic circular dichroism (XMCD) study of a 5.4 at. % Co-doped indium tin oxide (ITO) thin film shown to exhibit ferromagnetism beyond room temperature. The XAS spectra at the Co $L_{2,3}$ edge reveal pronounced multiplet features characteristic of divalent octahedrally coordinated $Co^{2+}$ ions. The results suggest that the $Co^{2+}$ ions are nonmetallic and substitute for the In site in ITO. Magnetic field and temperature-dependent XMCD spectra imply that the $Co^{2+}$ ions give a paramagnetic contribution to the overall ferromagnetic response both at the near-surface region and throughout the bulk of the films. No magnetic polarization was detected at the In $M_{2,3}$ or Sn $M_{2,3}$ edges. We therefore presume that the ferromagnetism observed is a result of the *sp-d* exchange interaction between the *sp* band of the host ITO and that of the localized *d* electrons of the transition-metal Co dopants.

DOI: 10.1103/PhysRevB.82.144429 PACS number(s): 75.47.Lx, 75.76.+j, 75.50.Pp

## I. INTRODUCTION

Dilute magnetic oxides (DMOs), formed when magnetic transition-metal (TM) ions are randomly substituted at host oxide lattice sites, are proving to be one of the most puzzling and interesting classes of magnetic materials that have emerged in recent years. These materials may exhibit ferromagnetism above room temperature suitable for next-generation spintronics-based multifunctional devices.[1] An ideal intrinsic DMO exhibits ferromagnetism as a result of a coupling interaction between localized moments at the substituted sites mediated by charge carriers of the host oxide. A number of oxide thin films have been reported to exhibit ferromagnetic behavior near or above room temperature but these results remain controversial and are often not reproducible due to their highly sensitive dependence on the deposition process and postdeposition treatment and storage. Several theoretical predictions and models have been proposed in recent years in an attempt to improve the understanding of the magnetic interactions within these systems.[2–5] However, given the detection of ferromagnetic behavior in undoped oxides,[6] further refinements to these models are clearly needed.[7]

Defects appear to play a crucial role in the development of ferromagnetism in these systems.[8] However, the exact role and contribution to the underlying mechanism of the defects in stabilizing ferromagnetism is yet to be established. Defects may include oxygen and cationic vacancies, as well as interstitial ions.

Tin (Sn)-doped indium oxide ($In_2O_3$) (ITO) (90 In:10 Sn) is an important functional transparent conducting oxide, which is the basis for the developing field of transparent electronics.[9] Reports of room-temperature ferromagnetism and magnetoresistance in transparent TM-doped $In_2O_3$ and ITO thin films[10–14] have sparked interest in their use in devices based on spin transport.

In order to achieve successful implementation of these materials in the spintronics field it is necessary that the carriers within the system are capable of becoming spin polarized, i.e., an *s*(*p*)-*d* exchange interaction between the *sp* band of the host oxide and that of the localized *d* electrons of the TM dopant. With the assurance that this is in fact the case, then a DMO is regarded as an *intrinsic* DMO. The observation of the anomalous Hall effect (AHE) is usually considered strong evidence for intrinsic ferromagnetic behavior in DMOs given its strong dependence on the spin-orbit interaction. However, the AHE has also been reported to arise in the presence of Co clusters,[15] and so is no longer considered an "acid test" for intrinsic ferromagnetism in DMOs.[16]

X-ray magnetic circular dichroism (XMCD), the difference in core-level absorption between right ($\rho_+$) and left ($\rho_-$) circularly polarized x rays, is an element- and site-specific probe of magnetism.[17] It uniquely enables the particular magnetic properties of the substituted TM ions in ITO to be studied. Since the absorption of polarized light leads to spin selectivity, ($\rho_+$) or ($\rho_-$) light preferentially probes the spin-up and spin-down states above the Fermi level. Further, the XMCD sum rules[18] can be applied to separate the contribution of spin and orbital contributions to the magnetic moment.[19] XMCD therefore provides a direct probe of the nature of ferromagnetism in DMOs. The majority of previous element-specific XMCD measurements at the Co $L_{2,3}$ edges have been performed on $Zn_{1-x}Co_xO$ thin films.[20–24] A detailed study on the local structural environment of Co in Co-doped ITO showed that below a Co doping level of 7 at. % the material system is free from metallic Co clustering and Co enters the ITO matrix via the substitution of In

 

atoms.[25] However, to date, no such advanced element-specific techniques such as XMCD have been used to investigate TM-doped ITO films.

In this report we have performed extensive studies using x-ray absorption spectroscopy (XAS) and XMCD of the In, Sn, and Co absorption sites in Co-doped ITO thin films, which are shown to exhibit ferromagnetic properties above room temperature. In particular, we have focused our attention on a 5.4 at. % Co-doped ITO film. Within the sensitivity limits of the techniques employed, we show that the In and Sn sites show no evidence of magnetic polarization and that the In-substituted Co sites provide a purely paramagnetic contribution to the overall magnetization.

## II. EXPERIMENTAL DETAILS

A series of Co-doped ITO $[In_{2-x}Sn_{x-1}(Co_x)O_{3-2x}$ with $x=0.016-0.054]$ thin films (250 nm thick) were deposited on *r*-plane sapphire substrates by dc magnetron sputtering in a UHV system. The substrates were maintained at a temperature of 350 °C during deposition. The system base pressure was better than $1\times10^{-6}$ Pa. Films were sputtered in $1.2\pm0.01$ Pa of an Ar-$O_2$ (95:5) mix (0.06 Pa $O_2$). Phase identification and structural properties of the Co-doped ITO were analyzed using x-ray diffraction (XRD) on a Bruker diffractometer in the $\theta$-$2\theta$ mode using Cu $K\alpha$ radiation. Compositional analysis was performed using energy-dispersive x-ray spectroscopy. A superconducting quantum interference device (SQUID) magnetometer was employed for characterization of the bulk magnetic properties. The samples were handled using nonmagnetic tweezers and mounted in the most common way using a plastic straw fastened using Kapton tape. These components were measured alone within the SQUID system and consistently produced a diamagnetic response. Measurements were performed in the temperature range of 2–300 K in magnetic fields up to 0.5 T. XAS and XMCD measurements were performed on beamline I06 at Diamond Light Source using the UHV compatible three-dimensional-vector superconducting high-field magnet with fields up to $\pm6$ T and temperature range between 2 and 370 K. The sample was mounted onto a custom-designed pure Cu block using silver paste for good electrical contact. All magnetic characterization was performed before any XAS or XMCD measurements were performed.

## III. RESULTS

Figure 1 shows the $\theta$-$2\theta$ XRD scans of Co-ITO films grown on *r*-plane sapphire for a range of Co doping levels. All peaks displayed on the diffractogram could be indexed assuming the same cubic bixbyite structure as pure ITO. Peaks were sharp, suggesting that the film is highly crystalline. At first glance, no detectable peaks corresponding to any secondary Co oxides or Co metal were found. This is often the case in DMOs which appear to be phase pure and of high crystalline quality. In order to verify these findings, the integration time per point was raised to 100 s, a route also taken by Opel *et al.*[26] where they increased the integration further to 400 s. Still, with this adjustment and within

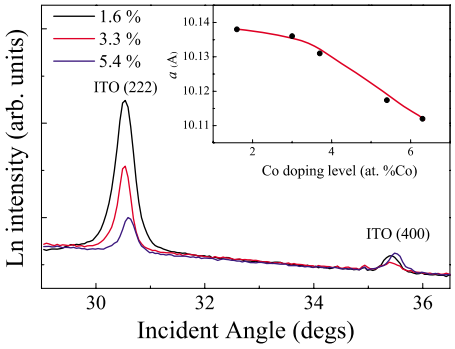


FIG. 1. (Color online) (a) $\theta$-$2\theta$ XRD diffractograms focusing on the ITO (222) and (400) for Co-ITO films of varying Co concentrations, demonstrating the shift in the peak position and intensity upon Co doping. Inset: Showing the steady decrease in the lattice parameter, $a$ (Å), as a function of Co doping. The solid line serves as a guide to the eyes.

the detection limit of the instrument, we were unable to identify any diffraction peaks which would suggest the presence of metallic Co clusters or any other secondary Co oxide phases. A shift in the peaks [predominantly the highly pronounced ITO (222) diffraction peak] toward higher values of $2\theta$ with increasing level of Co doping is seen and suggests a gradual decrease in the out-of-plane lattice parameter, $a$ (inset, Fig. 1). This is expected as the Co ions (e.g., $Co^{2+}$ ions have ionic radii of 0.74 Å, respectively, compared to 0.94 Å for $In^{3+}$) substitute for host In sites in the ITO lattice and suggests that the Co atoms are not forming clusters.

In-plane magnetization ($M$) versus field ($\mu_0 H$) measurements showed clear evidence for ferromagnetism in each of the samples. Figure 2(a) shows the magnetization loop for a 5.4 at. % Co-doped ITO film over a range of temperatures. Figure 2(b) provides a magnified view of the low-field data to demonstrate the nature of the coercive field and how it changes drastically between 2 and 300 K. The coercive field is seen to follow an inverse relationship with temperature [Fig. 2(c)], ranging from as high as ~70 mT at 2 K, falling to ~8 mT at 300 K. The diamagnetic background of the substrate and sample holder has been subtracted from all the magnetization data shown here. Maximum saturation magnetization was recorded to be 3.80 emu/cm$^3$ at 2 K, decreasing to 1.13 emu/cm$^3$ beyond room temperature for a 5.4 at. % Co-doped ITO film. Figure 2(d) shows the normalized field-cooled (FC) magnetization of the 5.4 at. % Co-doped ITO film as a function of temperature in a constant applied magnetic field of 0.5 T in the 5–300 K temperature range. The sample magnetization decreases rapidly particularly between 2–40 K where the magnetization has fallen by more than 50%. This implies that the sample possesses a strong paramagnetic component in addition to a weak ferromagnetic component, as seen in other DMO systems.[27] Initially, we attempted to fit the data using a purely paramagnetic relationship, however, this proved unsuccessful. Assuming that we have the coexistence of magnetic phases within this sample, we were able to model the magnetic susceptibility, $\chi$ (equivalent to $M/H$), using a modified Curie-Weiss relationship in combination with a standard mean-field model for a ferromagnet using the relation

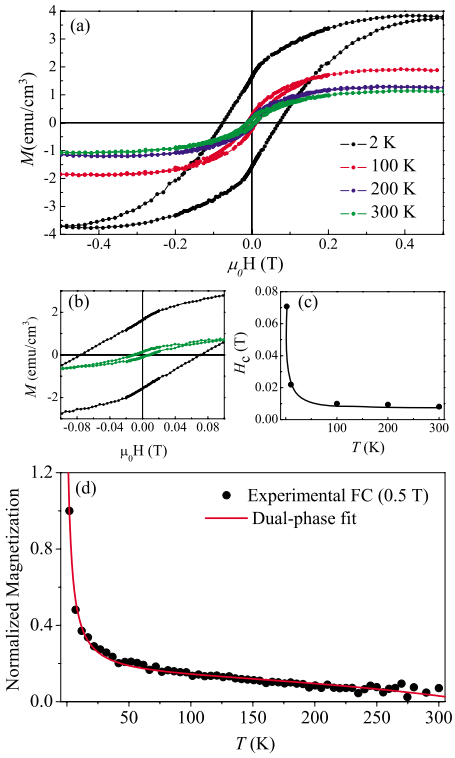


FIG. 2. (Color online) (a) Magnetic hysteresis loops using a SQUID magnetometer for a 5.4 at. % Co-doped ITO film at varying temperatures, (b) magnified image showing the large change in coercive field between 2 K (solid black circles) and 300 K (solid green circles), (c) variation in coercive field as a function of temperature; the solid line is a guide to the eyes, and, (d) normalized field-cooled magnetization for a 5.4 at. % Co-doped ITO film as a function of temperature in an applied magnetic field of 0.5 T; the solid line fits the experimental data to the magnetic dual-phase model described in Eq. (1).

$$\chi = [1-\alpha]\left(\chi_0 + \frac{C}{T+\theta}\right) + \alpha\sqrt{1-\frac{T^2}{T_c^2}}, \qquad (1)$$

where $\alpha$ is magnetic phase fraction (in this case, the ferromagnetic fraction), $\chi_0$ is a constant nonparamagnetic contribution to the magnetic susceptibility, $C$ is the Curie constant ($=n\mu^2/3k_B$, where $k_B$ is Boltzmann's constant), $\theta$ is the Curie-Weiss temperature and describes the magnetic interactions between the paramagnetic spins, $n$ number of magnetic ions and $\mu$ the magnetic moment of the ion, $T$ is the measurement temperature, and $T_c$ is the Curie temperature of the ferromagnet. The value for $\alpha$ is found to be 17%, confirming that the paramagnetic contribution is dominant in this sample. The fit estimates a $T_c$ of approximately 452 K. There was no sign of a blocking temperature, thus suggesting the absence of secondary Co metal nanoclusters within the bulk of the film. Zero-field-cooled/FC measurements using a 0.01 T applied field yielded the same result.

With a view to probe the magnetic nature of Co-doped ITO in greater detail, XAS and XMCD measurements were performed at the In $M_{2,3}$, Sn $M_{2,3}$, and Co $L_{2,3}$ edges. The sample surface orientation was set at 45° to the incident beam. The magnetic field, in all XMCD measurements here was applied in a direction parallel to the direction of the incident x-ray beam. The XAS spectra were recorded in both total-electron yield (TEY) and fluorescence yield (FY) modes in order to measure the surface and bulk components, respectively. TEY probes the sample with sampling depths of less than 10 nm and provides information representative of the near-surface region, whereas the FY can probe depths on the order of hundreds of nanometers.[28] For all measurements, a linear background fit to the pre-edge region was subtracted from the raw data and subsequently normalized by the maximum intensity of the specific-element peak of interest.

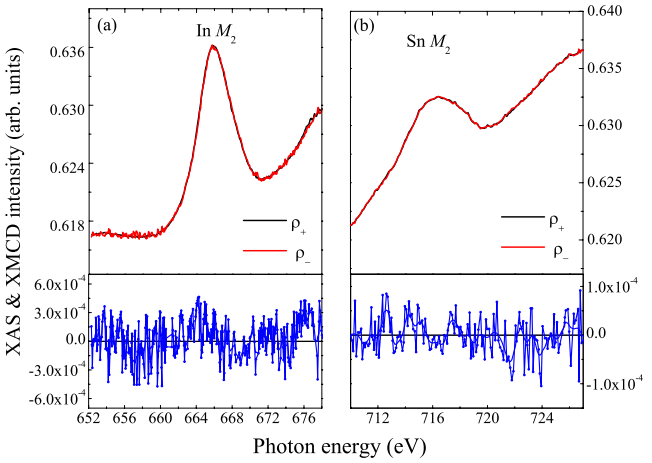


FIG. 3. (Color online) XAS and XMCD spectra in TEY mode at 2 K under an applied field of 4 T at the (a) In $M_2$ edge and (b) Sn $M_2$ edges, along with the raw XMCD data (solid circles) and a smoothed extrapolation (solid lines).

In order to investigate the possibility of magnetic polarization at the In and Sn lattice sites, XAS and XMCD spectra were recorded at the In $M_{2,3}$ and Sn $M_{2,3}$ edges. Both $In^{3+}$ and $Sn^{4+}$ have an electronic configuration of $4d^{10}$ and we would not expect any magnetic moment to be present at all. Figures 3(a) and 3(b) show the XAS and XMCD spectra measured in TEY at the In $M_2$ and Sn $M_2$ edges, respectively, at 2 K under an applied magnetic field of 4 T. No evidence of dichroic behavior at the In $M_2$ and Sn $M_2$ edges can be seen within the detection limits of the instrument. This excludes the presence of any detectable ferromagnetic polarization of the In $s$ and Sn $s$ and $d$ states. The same behavior was observed at both edges at 300 K also under an applied magnetic field of 4 T.

The XAS and XMCD spectra measured at 2 K in a 4 T field at the Co $L_{2,3}$ edge using TEY are shown in Fig. 4(a). The absorption edges appear due to a Co $2p \rightarrow 3d$ transition. This transition provides clues on the density of unoccupied Co $3d$ states, therefore probing the $3d$ magnetism of Co.[20] A large XMCD signal is present at the $L_3$ edge, indicating a significant magnetic moment at the $Co^{2+}$ sites in the applied magnetic field. The XMCD asymmetries $[(\rho_+ - \rho_-)/(\rho_+ + \rho_-)]$ at 2 K were estimated as 5.47% and 14.21%, respectively, for TEY and FY spectra. TEY is generally lower than FY and is consistent with the fact that there is a lower volume fraction of Co dopants and magnetic coupling near the surface region of the film. The pronounced multiplet struc-

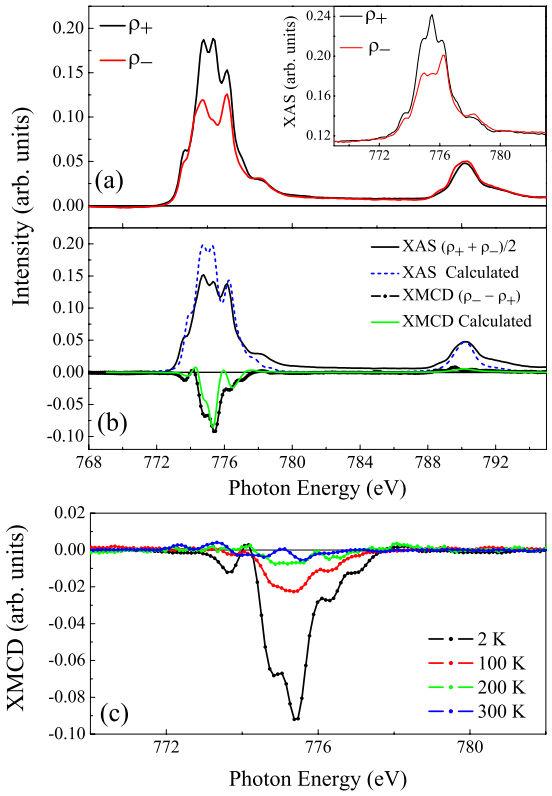


FIG. 4. (Color online) Co $L_{2,3}$ edge for a 5.4 at. % Co-doped ITO film at 2 K under an applied magnetic field of 4 T; (a) TEY XAS for right ($\rho_+$) and left ($\rho_-$) circularly polarized light. Inset: FY XAS spectra for right ($\rho_+$) and left ($\rho_-$) circularly polarized light under the same conditions, (b) average experimental TEY XAS and the calculated XAS spectra along with the experimental XMCD spectrum and calculated XMCD spectrum for octahedral $Co^{2+}(10D_q=0.7$ eV), (c) TEY XMCD spectra at the Co $L_2$ edge of a 5.4 at. % Co-doped ITO film as a function of temperature under an applied magnetic field of 4 T.

ture at the Co $L_{2,3}$ edges, which arises due to Coulomb and exchange interactions between the $2p$ core hole and $3d$ valence states, is typical of Co in a localized state. By comparing the XAS and XMCD spectra to those of metallic Co,[19] we conclude that Co clusters are absent in the surface region. The XAS recorded using FY mode [inset Fig. 4(a)] also exhibits pronounced multiplet features implying that the bulk of the film is also free from clustering and was true over the entire temperature range, where the multiplet features were maintained. The multiplet features observed are very similar to those reported in other Co-doped oxide systems.[20–24,29–31] Furthermore, the fine structure of the XMCD spectra appears to be maintained as the temperature approaches room temperature and is shown in Fig. 4(c). This is contrary to that observed in Co-doped $(La,Sr)TiO_3$ where it was suggested that the gradual loss in fine structure could be interpreted as a signature of poor ionic behavior and could indicate the presence of metallic Co clusters.[31]

To corroborate the experimental results, the XAS and XMCD spectra were calculated for the octahedral site symmetry of the Co ion (assuming Co substitutes for $In^{3+}$). Figure 4(b) shows the calculated results, which are in excellent agreement with the experimental data. The spectra show the electric dipole allowed transitions between the ground-state Co $3d^7t_{2g}^5e_g^2(^4T_{1g})$ and the final-state $2p^53d^8$ configuration in octahedral symmetry with crystal-field parameter $10D_q=0.7$ eV split by first-order spin-orbit interaction and in the presence of a magnetic exchange field of $g\mu_BH=1$ meV, where $g$ is the spectroscopic splitting factor (set as 2.0023 for free electrons), $\mu_B$ is the Bohr magneton, and $H$ is the applied magnetic field. The wave functions of ground and final states were calculated in intermediate coupling using Cowan's Hartree-Fock (HF) code with relativistic correction following the method described in Ref. 32. The Slater and spin-orbit parameters were as tabulated in Refs. 32 and 33. Interatomic screening and mixing was taken into account by reducing the atomic values of the Slater integrals $F_k(3d,3d)$, $F_k(2p,3d)$, and $G_k(2p,3d)$ to 70%, 80%, and 65%, respectively. The $2p$ spin-orbit interaction was scaled to 97% of the HF value. The calculated line spectra were broadened by a Lorentzian of $\Gamma=0.1$ (0.4) eV for the $L_3(L_2)$ edge to account for intrinsic linewidth broadening and a Gaussian of $\sigma=0.2$ eV for the instrumental broadening.

Element-specific magnetization curves were recorded using XMCD in TEY and FY mode at 2, 100, 200, and 300 K by sweeping the magnetic field and maintaining the incident photon energy at 777.3 eV. Figure 5(b) shows the magnetization curve measured in FY mode at 2 K. Note that this measurement does not give an absolute value for the moment on an individual $Co^{2+}$ ion but provides an indication of the field dependence of the Co moment in 5.4 at. % Co-doped ITO. Similar results were obtained in TEY mode, confirming that we observe no difference in the magnetic properties of the surface and throughout the bulk of the sample. The curve can be modeled well with a Brillouin function [Eq. (2)] to describe paramagnetic behavior, where $y=g\mu_BJH/k_BT$ and $M_0$ is the saturation magnetization. The curve shows no ferromagnetic or remanent behavior for the $Co^{2+}$ ions at any of the given temperatures. The fit yields a total angular momentum, $J$, of 0.761 and an effective magnetic moment $p=g[S(S+1)]^{1/2}$ of $2.32\mu_L$/Co,

$$M = M_0\left\{\left(\frac{2J+1}{2J}\right)\coth\left[\frac{(2J+1)y}{2J}\right] - \left(\frac{1}{2J}\right)\coth\left(\frac{y}{2J}\right)\right\}. \quad (2)$$

This value is lower, but within reasonable agreement, than the recorded value expected for paramagnetic Co ions in the upper spin state [+2 for electrons with spin $S=3/2$, giving 3.87 $\mu_B$ (Ref. 34)].

Figure 5(a) shows the respective XAS and XMCD spectra in FY mode at the Co $L_{2,3}$ edge at 300 K in the remanent state (0 T). The sample was first magnetized at 4 T before being ramped down to 0 T for measuring. No XMCD signal could be detected which is consistent with the XMCD magnetization curve discussed above, where no remanent XMCD effect is expected. The same was seen in the TEY measurements. Therefore, we can conclude that the specific contribution of Co $3d$ ions to the total bulk ferromagnetism measured in 5.4 at. % Co-doped ITO is purely paramagnetic, i.e., we

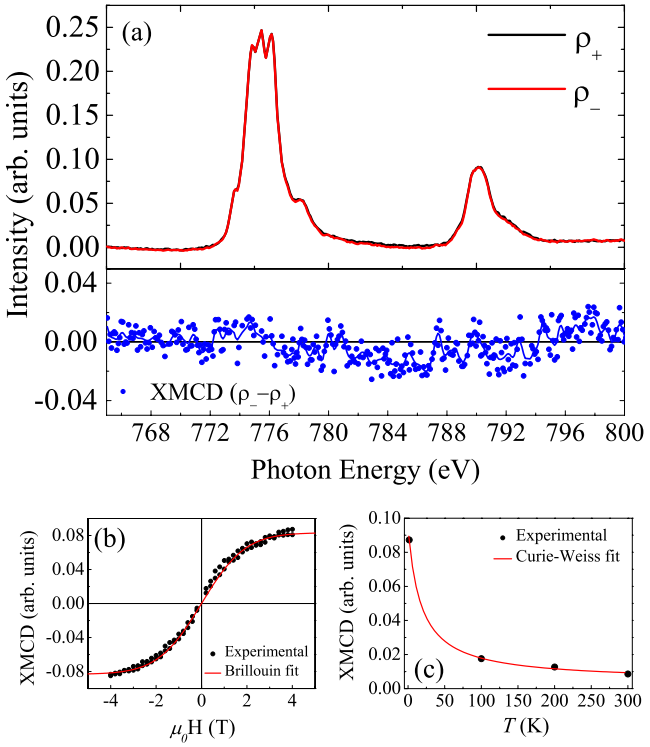


FIG. 5. (Color online) (a) XAS and XMCD spectra at the Co $L_{2,3}$ edge in FY mode at remanence (0 T) and 300 K. The XMCD is shown in the lower panel (solid circle with solid line), (b) Magnetization curve of a 5.4 at. % Co-doped ITO measured at the Co $L_{2,3}$ edge in FY mode at 2 K (solid circles), along with the fit to a Brillouin function (solid line), and (c) temperature dependence of the FY XMCD signal at an applied magnetic field of 4 T (solid circles), along with the fit to a modified Curie-Weiss law (solid line).

can assume that the Co ions are not exchange coupled with each other.

The temperature dependence of the XMCD measured in FY for the $Co^{2+}$ ions in an applied field of 4 T is shown in Fig. 5(c) and follows a modified Curie-Weiss law. This fit yields a Curie-Weiss temperature of $-13 \pm 4$ K, implying very weak antiferromagnetic coupling. From these findings, we conclude that there is strong evidence that the Co ions are not directly responsible for the ferromagnetism observed in the film.

Copie *et al.* also observed a similar "*s*-like" shaped XMCD magnetization curve, much like the data presented in Fig. 5(b). They, however, observe some anisotropy and claim that this may indicate ferromagnetic behavior regardless of the fact that there is no hysteresis. Together with the metallic-like Co XMCD spectra, they suggest a non-negligible contribution to the magnetic signal arising from Co clusters in a metallic state. Rode *et al.* also measured a closed XMCD magnetization loop in their $Zn_{0.95}Co_{0.05}O$ film but analysis at the Co *K* edge revealed the coexistence of two magnetic phases: a paramagnetic phase associated with ionic Co and an extrinsic ferromagnetic phase associated with Co metal clusters. We believe that the preservation of the multiplet line structure in the XMCD spectra and paramagnetic dependence of the XMCD signal over the entire temperature range

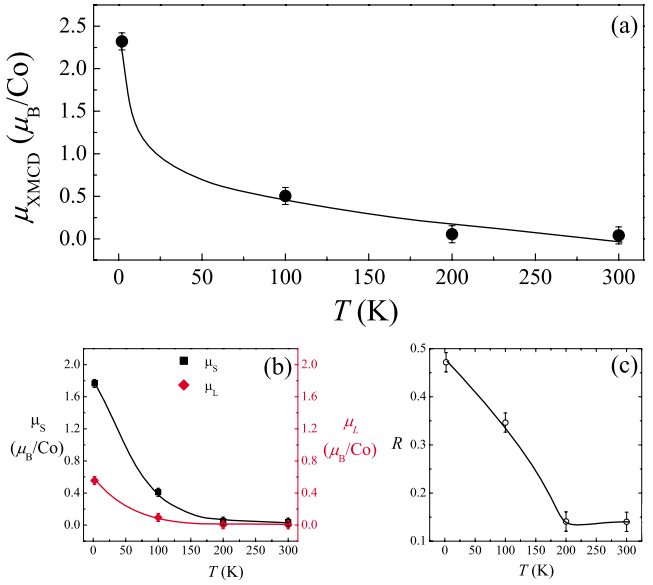


FIG. 6. (Color online) (a) Temperature dependence of calculated magnetic moment ($\mu_{XMCD}$) using normalized TEY XMCD spectrum and the application of the XMCD sum rules, (b) temperature dependence of the orbital ($\mu_L$) and spin ($\mu_S$) magnetic moments, and (c) temperature dependence of the ratio of the integrated signals over the $L_{2,3}$ edges, *R*. The solid lines are a guide to the eyes.

up to 300 K, is good evidence to suggest that within the detection limits of our instruments, metallic Co clusters are not present within our system.

Quantitative information regarding the orbital ($\mu_L$) and spin ($\mu_S$) components to the total magnetic moment ($\mu_{XMCD}$) were calculated by applying the sum rules,[18,19] where we have included the magnetic dipole term $\langle \mu_T \rangle$, with their dependence on temperature shown in Figs. 6(a) and 6(b). We have assumed a pure $3d^7$ configuration for the Co atoms, which sets the number of holes in the $3d$ shell to 3. Values for $\mu_{XMCD}$ are taken at an applied magnetic field of 4 T in TEY mode. The magnitude of $\mu_L$ and $\mu_S$ relatively high in comparison to some reports with comparable levels of Co doping in ZnO.[22,23] This could be due to the different crystal-field effects on the $Co^{2+}$ ions in the ITO matrix. The value for $\mu_{XMCD}$ at 2 K (2.32 $\mu_B$/Co) calculated from the sum rules is in excellent agreement with that estimated using the Brillouin fit in Fig. 5(b).

The expectation values of the orbital, $\mu_L$ and spin, $\mu_S$, moment along with the magnetic dipole term, $\mu_T$, are closely related by the sum rules to the integrated XMCD signal, as described by Gambardella *et al.*[35] The ratio, *R*, given by

$$R \equiv \frac{\mu_L}{\mu_S + \mu_T} = \frac{2}{3}\frac{\Delta A_3 + \Delta A2}{\Delta A_3 - 2\Delta A_2}, \tag{3}$$

where $\Delta A_3$ and $\Delta A_2$ are the integrated XMCD signals over the $L_{2,3}$ edges, respectively. Using this relationship with a $d^7$ ground state for Co, we find a discrepancy between the experimental value (0.48 at 2 K to 0.14 at 300 K) and theoretical (1.5) values for *R*. The trend in *R* as a function of the temperature is shown in Fig. 6(c). The striking rise in *R* as the temperature is lowered is a consequence of the Boltz-

mann population of spin-orbit levels in the ground state.[30]

The data recorded in FY mode are qualitatively similar. However, due to self-absorption effects which affect the relative intensity of $L_{2,3}$ peak, along with the differences in the matrix elements and selections rules for TEY and FY, application of the XMCD sum rules is meaningless here. They do, however, qualitatively confirm the absence of Co clusters throughout the bulk of the film and the decreasing magnetic moment with increasing temperature.

## IV. DISCUSSION

We have studied the origin of magnetic ordering in the Co-doped ITO system. The line shape of both the XAS and XMCD spectra we obtain show clear multiplet features over a wide range of temperatures suggesting that we have Co existing in an ionic state. The absence of dichroism at remanence at the Co $L_{2,3}$ edge and the modeling of the XMCD magnetization loops using a Brillouin function points toward paramagnetic behavior thus excluding their significant contribution to the ferromagnetism. This is supported further by the clear difference in comparison to the SQUID magnetometry measurements. In contrast to the XMCD magnetization loop at 2 K, the magnetic hysteresis loop shows a curve with saturation field of approximately 0.4–0.5 T with a large coercive field. The XMCD magnetization curve only shows signs of saturating beyond our measurement range of 4 T. This clearly shows that the two techniques are probing different phenomena and at the same time complementing each other in trying to determine the origins of the ferromagnetism in our samples.

These results suggest that the ferromagnetism we observe in Co-doped ITO is not related to the 3*d* electronic states. This is rather contradictory to what has been assumed to account for the magnetic properties in the DMO systems by those who have applied theoretical models to explain the unexpected behavior. These findings may point toward the likelihood that the bulk ferromagnetism observed from the SQUID magnetometry measurements may be oxygen-mediated, e.g., oxygen vacancies or oxygen-induced defects. Oxygen *K*-edge XAS data will certainly be capable of providing useful information on whether the features could be signatures of oxygen related lattice defects. Certain atomic defects in structures, such as oxygen vacancies with trapped electrons or holes, may contain low-lying triplet states that are capable of overlapping to form an impurity band.[36] These magnetic defects may interact through long-range interactions mediated by the impurity band to create a ferromagnetic ground state.[5] Therefore, further studies are required to definitively observe dichroism at oxygen sites at remanence. This would confirm the presence of a spontaneous ferromagnetic contribution.

## V. SUMMARY AND CONCLUSIONS

In summary, we have used XAS and XMCD at the In $M_{2,3}$, Sn $M_{2,3}$, and Co $L_{2,3}$ edges within Co-doped ITO to study the origin of the magnetism over a range of temperatures and applied magnetic fields. Element-specific hysteresis loops recorded at the Co $L_{2,3}$ edge indicate a clear paramagnetic contribution to the overall magnetic moment of the Co-doped ITO film and confirm the presence of noncoupled $Co^{2+}$ ions substituting for the In ions. Multiplet features in the Co $L_{2,3}$ edge XAS measured in both TEY and FY mode from 2 to 300 K indicate that the Co atoms are in a divalent state, therefore nonmetallic in nature throughout the entire film, and thus substituting for the In ions. The apparent absence of metallic Co clusters throughout the film is also supported from magnetometry and structural characterization techniques. Therefore, within the detection limits of the techniques, and from all the information we have through our exhaustive characterization efforts, we believe that there is no contribution to the observed ferromagnetism solely from the Co dopants. No XMCD could be detected at the In $M_2$ or Sn $M_2$ edge, thus excluding the presence of a large magnetic polarization of the In and Sn sublattices. The ferromagnetic moment observed in the Co-doped ITO films can therefore not be ascribed to the Co and In sublattices. We propose an oxygen-mediated ferromagnetic response and, therefore, future studies will be directed toward detailed experiments at the oxygen *K* edge in order to refine our findings.

## ACKNOWLEDGMENTS

We would like to thank Richard Mott for his support during the experiments at Diamond Light Source and the Science and Technology Facilities Council for access to the SQUID instrument. A.M.H.R.H thanks G. A. Gehring for many helpful discussions and L. J. Pearson for editorial input. This research was funded by the UK Engineering and Physical Sciences Research Council.

*amh74@cam.ac.uk

[1] H. Ohno, Science **281**, 951 (1998).
[2] T. Dietl, H. Ohno, F. Matsukura, J. Cibert, and D. Ferrand, Science **287**, 1019 (2000).
[3] T. Dietl, H. Ohno, and F. Matsukura, Phys. Rev. B **63**, 195205 (2001).
[4] A. Kaminski and S. Das Sarma, Phys. Rev. Lett. **88**, 247202 (2002).
[5] J. M. D. Coey, M. Venkatesan, and C. B. Fitzgerald, Nature Mater. **4**, 173 (2005).
[6] J. M. D. Coey, Solid State Sci. **7**, 660 (2005).
[7] J. M. D. Coey and S. A. Chambers, MRS Bull. **33**, 1053 (2008).
[8] B. Ali, L. R. Shah, C. Ni, J. Q. Xiao, and S. I. Shah, J. Phys.: Condens. Matter **21**, 456005 (2009).
[9] J. W. Seo, J.-W. Park, K. S. Lim, J.-H. Yang, and S. J. Kang, Appl. Phys. Lett. **93**, 223505 (2008).
[10] J. Stankiewicz, F. Villuendas, and J. Bartolomé, Phys. Rev. B **75**, 235308 (2007).

[11] H. S. Kim, S. H. Ji, H. Kim, S.-K. Hong, D. Kim, Y. E. Ihm, and W. K. Choo, Solid State Commun. **137**, 41 (2006).
[12] J. Philip, A. Punnoose, B. I. Kim, K. M. Reddy, S. Layne, J. O. Holmes, B. Satpati, P. R. LeClair, T. S. Santos, and J. S. Moodera, Nature Mater. **5**, 298 (2006).
[13] X. L. Wang, G. Peleckis, S. X. Dou, R. S. Liu, and J. G. Zhu, J. Appl. Phys. **101**, 09H121 (2007).
[14] J. Philip, N. Theodoropoulou, G. Berera, J. S. Moodera, and B. Satpati, Appl. Phys. Lett. **85**, 777 (2004).
[15] S. R. Shinde, S. B. Ogale, J. S. Higgins, H. Zheng, A. J. Millis, V. N. Kulkarni, R. Ramesh, R. L. Greene, and T. Venkatesan, Phys. Rev. Lett. **92**, 166601 (2004).
[16] J. M. D. Coey, Curr. Opin. Solid State Mater. Sci. **10**, 83 (2006).
[17] G. Schütz, W. Wagner, W. Wilhelm, P. Kienle, R. Zeller, R. Frahm, and G. Materlik, Phys. Rev. Lett. **58**, 737 (1987).
[18] B. T. Thole, P. Carra, F. Sette, and G. van der Laan, Phys. Rev. Lett. **68**, 1943 (1992).
[19] C. T. Chen, Y. U. Idzerda, H.-J. Lin, N. V. Smith, G. Meigs, E. Chaban, G. H. Ho, E. Pellegrin, and F. Sette, Phys. Rev. Lett. **75**, 152 (1995).
[20] T. Tietze, M. Gacic, G. Schütz, G. Jakob, S. Brück, and E. Goering, New J. Phys. **10**, 055009 (2008).
[21] M. Kobayashi, Y. Ishida, J. l. Hwang, T. Mizokawa, A. Fujimori, K. Mamiya, J. Okamoto, Y. Takeda, T. Okane, Y. Saitoh, Y. Muramatsu, A. Tanaka, H. Saeki, H. Tabata, and T. Kawai, Phys. Rev. B **72**, 201201(R) (2005).
[22] M. Gacic, G. Jakob, C. Herbort, H. Adrian, T. Tietze, S. Brück, and E. Goering, Phys. Rev. B **75**, 205206 (2007).
[23] A. Barla, G. Schmerber, E. Beaurepaire, A. Dinia, H. Bieber, S. Colis, F. Scheurer, J.-P. Kappler, P. Imperia, F. Nolting, F. Wilhelm, A. Rogalev, D. Müller, and J. J. Grob, Phys. Rev. B **76**, 125201 (2007).
[24] K. Rode, R. Mattana, A. Anane, V. Cros, E. Jacquet, J.-P. Contour, F. Petroff, A. Fert, M.-A. Arrio, Ph. Sainctavit, P. Bencok, F. Wilhelm, N. B. Brookes, and A. Rogalev, Appl. Phys. Lett. **92**, 012509 (2008).
[25] G. Subías, J. Stankiewicz, F. Villuendas, M. P. Lozano, and J. García, Phys. Rev. B **79**, 094118 (2009).
[26] M. Opel, K.-W. Nielsen, S. Bauer, S. T. B. Goennenwein, J. C. Cezar, D. Schmeisser, J. Simon, W. Mader, and R. Gross, Eur. Phys. J. B **63**, 437 (2008).
[27] K. M. Reddy, J. Hays, S. Kundu, L. K. Dua, P. K. Biswas, C. Wang, V. Shutthanandan, M. H. Engelhard, X. Mathew, and A. Punnoose, J. Mater. Sci.: Mater. Electron. **18**, 1197 (2007).
[28] Y. U. Idzerda, C. T. Chen, H.-J. Lin, G. Meigs, G. H. Ho, and C.-C. Kao, Nucl. Instrum. Methods Phys. Res. A **347**, 134 (1994).
[29] N. R. S. Farley, K. W. Edmonds, A. A. Freeman, G. van der Laan, C. R. Staddon, D. H. Gregory, and B. L. Gallagher, New J. Phys. **10**, 055012 (2008).
[30] G. van der Laan, E. Arenholz, R. V. Chopdekar, and Y. Suzuki, Phys. Rev. B **77**, 064407 (2008).
[31] O. Copie, K. Rode, R. Mattana, M. Bibes, V. Cros, G. Herranz, A. Anane, R. Ranchal, E. Jacquet, K. Bouzehouane, M.-A. Arrio, P. Bencok, N. B. Brookes, F. Petroff, and A. Barthélémy, J. Phys.: Condens. Matter **21**, 406001 (2009).
[32] G. van der Laan and B. T. Thole, Phys. Rev. B **43**, 13401 (1991).
[33] G. van der Laan and I. W. Kirkman, J. Phys.: Condens. Matter **4**, 4189 (1992).
[34] S. Blundell, *Magnetism in Condensed Matter* (Oxford University Press, Oxford, 2001), p. 49.
[35] P. Gambardella, S. S. Dhesi, S. Gardonio, C. Grazioli, P. Ohresser, and C. Carbone, Phys. Rev. Lett. **88**, 047202 (2002).
[36] S. Krishnamurthy, C. McGuinness, L. S. Dorneles, M. Venkatesan, J. M. D. Coey, J. G. Lunney, C. H. Patterson, K. E. Smith, T. Learmonth, P.-A. Glans, T. Schmitt, and J.-H. Guo, J. Appl. Phys. **99**, 08M111 (2006).